Warmstarting strategies for convex optimization based multi-channel constrained active noise control filter design

Yongjie Zhuang[a)], Zhuang Mo[a)], Yangfan Liu[a)]

In real-world applications of active noise control (ANC) systems, various constraints are supposed to be satisfied in the controller design process. The optimal control filter coefficients can be obtained by solving a constrained optimization problem, which usually requires a significant computational effort. Recently, a convex formulation in conic form was proposed for ANC filter design. The proposed formulation was shown to result in a computational time reduction by several orders of magnitude. It is of great interest to further improve its efficiency by using a priori information of the optimal filter coefficients. One potential way of achieving this goal is to introduce a warmstart technique so that the filter solution of a similar system or environment can be referred to for selecting the starting point of the optimization algorithm. However, the conic formulation should be solved by the interior-point method (IPM), which, in general, is challenging for applying warmstart techniques. In the current work, relaxation methods are proposed to the constraints of original ANC filter design formulation so that the warmstart techniques can be applied. Then, a warmstarting technique proposed in previous study is used to solve a series of perturbed problems, and the performance of the warmstarting technique is investigated. Results show that with the proposed modifications applied, the warmstarting strategy can significantly reduce the number of iterations needed for solving the conic formulation of the ANC filter design problem without much tuning efforts and the method is effective and robust in various environmental setups.

Primary subject classification: 38.2; Secondary subject classification: 74.9

1 INTRODUCTION

In active noise control (ANC) filter design, various types of constraints on noise control filter coefficients may be needed. For example, the robust stability constraints, the filter response constraints, and disturbance enhancement constraints[1]. When one type of constraint is required, one commonly followed method of constrained ANC filter design is introducing a regularization term in the filter coefficient optimization process[1], which can be further extended to leaky FxLMS method[2,3]. When multiple types of constraints are required, filter coefficients obtained by solving a constrained optimization problem formulated using H_2/H_∞ method can usually achieve a better noise control performance[4] compared with leaky FxLMS method. However, the computational load in solving the constrained optimization problem can be significant especially when multi-channel systems are required to create a relatively larger quiet zone. The high demand in computational power becomes one of the challenges for constrained optimization-based ANC filter design method to be applied to commercial product design.

[a)] Mechanical Engineering/Ray W. Herrick Laboratories, Purdue University; corresponding author: Yangfan Liu, yangfan@purdue.edu

To improve the computational efficiency of constrained multi-channel ANC filter design based on constrained optimization, Zhuang and Liu proposed a convex optimization based multi-channel constrained ANC filter design method[4–7] and demonstrated that the computational time can be reduced significantly from the order of hours to seconds[4,7] compared with the traditional constrained optimization-based ANC design method. To further improve the computational efficiency of their proposed method, one potential approach is to choose an appropriate initial point based on the a priori information of the optimal filter coefficients (i.e., the warmstart methods). An initial point is required in ANC filter design due to the iterative nature of solving a constrained optimal ANC filter. So far, the cold start approach is commonly used, i.e., no a priori information of the filter design problem is considered while choosing the initial point. For example, one can start from origin when using the leaky FxLMS method, or start from identity point which is well centered inside the feasible set when using constrained optimization method[4,8,9]. In many ANC applications, a reasonable guess of the optimal filter coefficients may be obtainable. A good example is in the commercial product design, where some product models are variations of previous models, or a specific product is a variation to the prototype product due to the batch manufacture process error. In these cases, if the optimal filter coefficients of one product are known, it can be used as an initial guess when solving the optimal filter coefficients for other products. On the other hand, when the constrained optimization method is applied on time-varying applications, the optimization problem associated with current adaption iteration can be treated as a perturbed problem with respect to that of a previous adaption iteration. The optimal solutions of two adaptation iterations should be close to each other so the previous optimal solution can be used to obtain a warm-start initial point for the current iteration. The term "warmstarting method" refers to such an approach of selecting initial point using a priori information.

However, in the approach Zhuang and Liu proposed[4,7], the primal-dual interior-point method (PD-IPM) should be used to achieve the significant computational efficiency improvement. Warmstarting strategies are difficult in PD-IPM which can be illustrated in Fig. 1. In Fig. 1, suppose an optimal solution is obtained for the original optimization problem on the left side. And a new optimization problem on the right side which has the solid line as feasible set boundaries is a perturbation of the original optimization problem (with dashed line as the feasible set boundaries). Usually, a good initial point should fall near the central path shown in the figure to be away from the boundaries and inside the feasible set. And the optimal solution is always at the feasible boundaries because of the linear cost function. If the optimal solution of the original optimization problem is used as the initial guess for the perturbed optimization problem, it may be too close to the feasible set boundaries or even fall outside of the feasible set boundaries, which can cause severe numerical problems[8]. This limits the application of the previously proposed method in scenarios where approximate values of optimal filter coefficients are known. In previous studies, the warmstarting strategies for PD-IPM have been investigated. Xia[10] proposed a warmstarting strategy based on semismooth Newton's method, which requires the complementary conditions to be transformed into equations. In Gondzio and Grothey's work[11], a method that leads the iterations back to feasible region was proposed, relying on sensitivity analysis of the Newton step. Skajaa et al.[12,13] proposed a concise strategy using convex combination of the cold start point of the current problem and the optimal solution of a similar problem.

This article is an extension of the work previously presented at and published for a conference[14]. In this article, the convex formulation and its cone programming reformulation for multi-channel ANC filter

design problem proposed by Zhuang and Liu[4,7] is firstly adopted. Then, the warmstarting strategy for homogeneous and self-dual IPM proposed by Skajaa et al.[13] is followed, combined with the cold start initial point used in SDPT3[15], as the warm-starting method for (convex) conic form ANC optimization problem. The strategy proposed by Skajaa[13] is mainly used for linear programming (LP) and second-order cone (SOC) programming, but the conic form ANC problem proposed by Zhuang and Liu[4,7] contains positive semidefinite (PSD) cones reformulated from the stability and robustness constraints. Thus, two methods of reformulating stability and robustness constraints into SOC are also proposed in this article. A set of system responses data measured from an experimental setup is used as the original problem whose optimal coefficients are used for choosing the warmstarting point. The perturbed problems are system responses changed by randomly changing the primary noise characteristics, the secondary path responses, or the acoustic feedback path responses. The warmstarting performance of using different warmstarting ratios on problems with different perturbation ratios is also investigated. The result demonstrated that compared with solving ANC optimization problem with mixed SOC and PSD cones, the warmstarting strategy has a better performance when solving the ANC optimization problem with only SOC. And the results showed that the applied warmstarting method can successfully reduce significant amounts of iterations compared with the cold start method when the proposed reformulation is applied, and it is effective and robust.

2 Theory

In this section, the multiple-input-multiple-output (MIMO) ANC control system, the H_2/H_∞ framework formulation for constrained optimal filter design, and the convex/conic formulation for improving computational efficiency are reviewed. The formulation in this article is based on a feedforward control structure. The feedback control structure can be formulated in a similar way if an internal model control structure (IMC) is used[16]. The variables used in this article are listed in Table 1.

2.1 ANC System Diagram and Notation

The MIMO ANC feedforward control diagram is shown in Fig. 2. There are N_r microphones, N_s loudspeakers, and N_e microphones used as reference sensors, secondary sources, and error sensors respectively. $\vec{\mathbf{x}}$ denotes the primary sound field signals at reference sensor locations. $\vec{\mathbf{r}}$ denotes the signal obtained from the reference microphones when the ANC system is activated. $\vec{\mathbf{y}}$ is the output of the ANC controller. $\vec{\mathbf{d}}_e$ is the disturbance signal. $\vec{\mathbf{e}}$ denotes the error signal, which is attenuated by the ANC system. $\mathbf{G}_{s_0}$ is the acoustic feedback path matrix that represents the acoustic responses of secondary sources at the reference sensors. To estimate the primary noise signals, $\vec{\mathbf{x}}$, from the reference signals $\vec{\mathbf{r}}$, an internal model cancellation (IMC) structure is used to cancel the acoustic feedback path effect[1,16,17]. When $\widehat{\mathbf{G}}_{s_0}$, a model of the physical feedback path $\mathbf{G}_{s_0}$, is assumed to be a perfect model, i.e., $\widehat{\mathbf{G}}_{s_0} = \mathbf{G}_{s_0}$, this system is simplified to a standard feedforward system as shown in Fig. 3. $\mathbf{G}_e$ represents the acoustical responses matrix of the secondary sources at the error sensor positions. $\mathbf{W}_x$ is the frequency response matrix of the multi-channel ANC FIR filters, $\mathbf{w}_F$, which need to be designed.

2.2 Review of Convex and Cone Formulation for ANC Design Problem

In practice, sometimes constraints on filter coefficients need to be satisfied while designing the control filter $\mathbf{w}_F$[16], such as robust stability constraints due to the closed loop formed by the acoustic feedback path and the noise control filters, the disturbance enhancement constraint to prevent noise amplification outside the noise control bands, and the filter response magnitude constraint to ensure the speaker operate in its linear response range. One of the commonly used design approaches is to solve a constrained optimization problem[16,17], which requires significant computational power. To reduce the computational load and to improve the numerical stability of this type of constrained optimization method, Zhuang and Liu[4,7] proposed a convex/cone formulation method. The formulation is briefly reviewed in this section, and more details can be found in references[4,7].

The multi-channel ANC filter design can be formulated as a convex optimization problem using the H_2/H_∞ framework with some relaxations and reformulations[4]:

$$\min_{\mathbf{w}_F} \quad \vec{\mathbf{w}}^{\mathrm{T}}\left(\sum_{k=1}^{N_f}\mathbf{A}_J(f_k)\right)\vec{\mathbf{w}} + \sum_{k=1}^{N_f}\vec{\mathbf{b}}_J^{\mathrm{T}}(f_k)\vec{\mathbf{w}} \tag{1.a}$$

$$\text{s.t.} \quad \vec{\mathbf{w}}^{\mathrm{T}}\mathbf{A}_J(f_k)\vec{\mathbf{w}} + \vec{\mathbf{b}}_J^{\mathrm{T}}(f_k)\vec{\mathbf{w}} + \tilde{c}_J(f_k) \le 0, \tag{1.b}$$

$$\left\|\vec{\mathbf{F}}_z^{\mathrm{T}}(f_k)\vec{\mathbf{w}}_{F_{i,j}}\right\|_2 - C_{i,j}(f_k) \le 0, \tag{1.c}$$

$$\max\left(\lambda\left(\frac{\mathbf{A}_S + \mathbf{A}_S^{\mathrm{H}}}{2}\right)\right) - (1-\epsilon_s) \le 0, \tag{1.d}$$

$$\max\big(\sigma(\mathbf{A}_S)\big)B(f_k) - 1 \le 0, \tag{1.e}$$

for all frequency points f_k, controller output channel index i, and controller input channel index j. $\vec{\mathbf{w}}$ is a vector containing all filter coefficients of each channel of control filter $\mathbf{w}_F$:

$$\vec{\mathbf{w}} = \left[\vec{\mathbf{w}}_{F_{1,1}}^{\mathrm{T}}, \ldots, \vec{\mathbf{w}}_{F_{1,N_r}}^{\mathrm{T}}, \vec{\mathbf{w}}_{F_{2,1}}^{\mathrm{T}}, \ldots, \vec{\mathbf{w}}_{F_{N_S,N_r}}^{\mathrm{T}}\right]^{\mathrm{T}}, \tag{2}$$

where N_S is the number of controller output channels (i.e., secondary sources), N_r is the number of controller input channels (i.e., reference sensors). The objective function Eqn. (1.a) is the total power of error signals across all desired frequencies, which can be further reformulated as a SOC in the cone programming formulation[7]. The expressions for $\mathbf{A}_J(f_k)$ and $\vec{\mathbf{b}}_J(f_k)$ are[4]:

$$\mathbf{A}_J(f_k) = \Re\left(\left(\mathbf{G}_e^{\mathrm{H}}(f_k)\mathbf{G}_e(f_k)\right) \otimes \mathbf{S}_{xx}^{\mathrm{T}}(f_k) \otimes \left(\vec{\mathbf{F}}_z^{*}(f_k)\vec{\mathbf{F}}_z^{\mathrm{T}}(f_k)\right)\right), \tag{3.a}$$

$$\vec{\mathbf{b}}_J(f_k) = 2\Re\left(\mathrm{vec}\left(\left(\mathbf{S}_{xd_e}(f_k)\mathbf{G}_e(f_k)\right) \otimes \vec{\mathbf{F}}_z(f_k)\right)\right), \tag{3.b}$$

where $\mathbf{S}_{xx}(f_k)$ is the cross-spectral density matrix of $\vec{\mathbf{x}}$ and $\mathbf{S}_{xd_e}(f_k)$ is the cross-spectral density matrix between $\vec{\mathbf{x}}$ and $\vec{\mathbf{d}}_e$; $\vec{\mathbf{F}}_z(f_k)$ is the associated Fourier transform vector; T and H represent transpose and complex conjugate transpose respectively; $\Re()$ represents taking the real part of a complex number or matrix; $\otimes$ represents the Kronecker product; vec() converts a matrix to a vector by stacking the columns.

The constraint, Eqn. (1.b), is introduced to prevent large enhancement at some frequency band, where[7]

$$\tilde{c}_J(f_k) = \mathrm{tr}\left(\mathbf{S}_{d_e d_e}(f_k)\right)\left(1 - A_e(f_k)\right), \tag{4}$$

$\mathbf{S}_{d_e d_e}(f_k)$ is the cross-spectral density matrix of $\vec{\mathbf{d}}_e$ and $A_e(f_k)$ is specified as the upper bound of the enhancement ratio of error signals at frequency f_k[7]. Equation (1.c) is used to constrain the amplitude of the control filter response for each channel and $C_{i,j}(f_k)$ is the upper bound of frequency response magnitude of designed control filter of i-th output and j-th input channel. Both Eqn. (1.b) and Eqn. (1.c) can be further reformulated equivalently to SOC in conic formulation[7]. Even if $\widehat{\mathbf{G}}_{s_0} = \mathbf{G}_{s_0}$ in nominal operating condition, the robust stability of the closed loop formed by the controller and acoustic feedback path should be considered. Equation (1.d) and (1.e) are applied to ensure the stability and robustness of this closed loop, respectively, where

$$\mathbf{A}_s = -\mathbf{W}_x(f_k)\widehat{\mathbf{G}}_{s_0}(f_k), \tag{5}$$

$\lambda()$ and $\sigma()$ denote the eigenvalues and singular values of a matrix, $B(f_k)$ is the upper bound of the output multiplicative plant uncertainty at frequency f_k, and ϵ_s is a small positive number to ensure strict inequality constraints. Both Eqn. (1.d) and Eqn. (1.e) can be reformulated equivalently to positive-semidefinite (PSD) cones[5]. Thus, Eqn. (1.a)-(1.e) can be further reformulated to cone programming formulation[7]:

$$\begin{aligned} \text{min.} \quad & \vec{\mathbf{c}}^{\mathrm{T}}\vec{\mathbf{x}}_p \\ \text{s.t.} \quad & \mathbf{A}\vec{\mathbf{x}}_p = \vec{\mathbf{b}}, \\ & \vec{\mathbf{x}}_p \in K, \end{aligned} \tag{6}$$

where K is a Cartesian product of various SOC and PSD cones, $\vec{\mathbf{x}}_p$ is the variable, and $\mathbf{A}, \vec{\mathbf{b}}$, and $\vec{\mathbf{c}}$ are constant matrix and vectors. Eqn. (6) is the same equation to Eqn. (12) in Zhuang and Liu's previous work[7] and the expression of $\vec{\mathbf{x}}_p$, $\mathbf{A}, \vec{\mathbf{b}}$, and $\vec{\mathbf{c}}$ are given in Eqn. (7), (12), and Appendix C in Zhuang and Liu's previous work[7]. More details on this conic formulation are introduced in Zhuang and Liu's previous work[7].

2.3 Review of Warmstarting Strategy

The dual problem of Eqn. (6) is:

$$\begin{aligned} \text{max.} \quad & \vec{\mathbf{b}}^{\mathrm{T}}\vec{\mathbf{y}}_d \\ \text{s.t.} \quad & \mathbf{A}^{\mathbf{T}}\vec{\mathbf{y}}_d + \vec{\mathbf{s}}_d = \vec{\mathbf{c}}, \\ & \vec{\mathbf{s}}_d \in K, \end{aligned} \tag{7}$$

where $\vec{\mathbf{y}}_d$ is the dual variable associated with equality constraints in Eqn. (6) and $\vec{\mathbf{s}}_d$ is the dual variable associated with inequality (conic) constraints in Eqn. (6) (considering $\vec{\mathbf{x}}_p$ in Eqn. (6) to be the primal variable); the $\mathbf{A}$ and $\vec{\mathbf{b}}$ are the same matrix and vector as that in the primal problem Eqn. (6). To solve the optimization problem expressed with Eqn. (6), a homogeneous and self-dual model of Eqn. (6) and Eqn. (7) is formulated as[13]:

$$\begin{aligned} \text{min.} \quad & \theta\mu(z^0) \\ \text{s.t.} \quad & \mathbf{A}\vec{\mathbf{x}}_p - \vec{\mathbf{b}}\tau = \theta r_p(z^0), \\ & -\mathbf{A}^{\mathbf{T}}\vec{\mathbf{y}}_d - \vec{\mathbf{s}}_d + \vec{\mathbf{c}}\tau = \theta r_d(z^0), \\ & \vec{\mathbf{b}}^{\mathrm{T}}\vec{\mathbf{y}}_d - \vec{\mathbf{c}}^{\mathrm{T}}\vec{\mathbf{x}}_p - \kappa = \theta r_g(z^0), \\ & r_p(z^0)^{\mathrm{T}}\vec{\mathbf{y}}_d - r_d(z^0)^{\mathrm{T}}\vec{\mathbf{x}}_p + r_g(z^0)\,\tau = \mu(z^0), \\ & \left(\vec{\mathbf{x}}_p, \tau\right) \geq 0, (\vec{\mathbf{s}}_d, \kappa) \geq 0, (\vec{\mathbf{y}}_d, \theta) \text{ free}, \end{aligned} \tag{8}$$

where $z = (\vec{\mathbf{x}}_p, \tau, \vec{\mathbf{y}}_d, \vec{\mathbf{s}}_d, \kappa)$ are the variables (τ and κ are two additional variables to make the formulation self-dual), $z^0 = (\vec{\mathbf{x}}_p^0, \tau^0, \vec{\mathbf{y}}_d^0, \vec{\mathbf{s}}_d^0, \kappa^0)$ are the initial points, and

$$\begin{aligned} r_p(z) &= \mathbf{A}\vec{\mathbf{x}}_p - \vec{\mathbf{b}}\tau, \\ r_d(z) &= -\mathbf{A}^{\mathbf{T}}\vec{\mathbf{y}}_d - \vec{\mathbf{s}}_d + \vec{\mathbf{c}}\tau, \\ r_g(z) &= \vec{\mathbf{b}}^{\mathrm{T}}\vec{\mathbf{y}}_d - \vec{\mathbf{c}}^{\mathrm{T}}\vec{\mathbf{x}}_p - \kappa \\ \mu(z) &= \left(\vec{\mathbf{x}}_p^{\mathrm{T}}\vec{\mathbf{s}}_d + \tau\kappa\right)/(\nu + 1). \end{aligned} \tag{9}$$

We can notate the commonly used cold start point as z^c. In this article, $z^c = (\vec{\mathbf{x}}_p^c, \tau^c, \vec{\mathbf{y}}_d^c, \vec{\mathbf{s}}_d^c, \kappa^c)$ is chosen using the same strategy as in SDPT3[15], which is a point well centered in the feasible set. Then, the proposed warmstarting point can be calculated[13]:

$$\begin{aligned} \vec{\mathbf{x}}_p^0 &= g\vec{\mathbf{x}}_p^* + (1-g)\vec{\mathbf{x}}_p^c, \\ \vec{\mathbf{s}}_d^0 &= g\vec{\mathbf{s}}_d^* + (1-g)\vec{\mathbf{s}}_d^c, \\ \vec{\mathbf{y}}_d^0 &= g\vec{\mathbf{y}}_d^*, \\ \tau^0 &= \tau^c, \\ \kappa^0 &= \vec{\mathbf{x}}_p^{0\,\mathrm{T}}\vec{\mathbf{s}}_d^0/n, \end{aligned} \tag{10}$$

where $\vec{\mathbf{x}}_p^*$, $\vec{\mathbf{s}}_d^*$, and $\vec{\mathbf{y}}_d^*$ are known optimal solutions (i.e., the a priori information) of a similar (or perturbed) optimization problem. $0 \le g \le 1$ is the warm ratio representing the relative location of the warmstarting point between the optimal solution of a similar optimization problem and the cold start point of the current optimization problem. n is the dimension of variable $\vec{\mathbf{x}}_p$ or $\vec{\mathbf{s}}_d$. A graphical illustration of this warmstarting is shown in Fig. 4. The warm ratio essentially interpolates a point in between the cold start point and the optimal point from a similar optimization problem such that it falls inside the feasible set and is near the central path to prevent numerical issues, while the interpolated point (warmstart point) is also closer to the new optimal point to reduce the required iterations. One advantage of this warmstarting method is that the required computational effort is small, and no iterative process is involved. Thus, this warmstarting strategy has good numerical efficiency and stability.

2.4 Proposed Constraint Modification

The warmstarting methods are usually applied to cone programming problem with SOC only in previous studies[13]. For the ANC filter design problem, PSD cones exist because of the robust stability constraint, which is one of the most essential constraints. In this section, two different relaxations are proposed to relax the PSD cones to SOC. In the following derivation, although the PSD cone is relaxed to SOC, it is achieved by replacing the original stability or robust constraint function with a more restrictive function.

First, robust stability constraints Eqn. (1.d) and Eqn. (1.e) are satisfied if the following holds[4]:

$$\left\|\mathbf{W}_x(f_k)\widehat{\mathbf{G}}_{s_0}(f_k)\right\|_2 \le \min\{1-\epsilon_s, 1/B(f_k)\}. \tag{11}$$

A very conservative relaxation is to consider that the max-norm of an arbitrary $m \times n$ matrix $\mathbf{M}$ satisfies:

$$\|\mathbf{M}\|_2 \le \sqrt{mn}\|\mathbf{M}\|_{\max}. \tag{12}$$

Thus,

$$\left\|\mathbf{W}_x(f_k)\widehat{\mathbf{G}}_{s_0}(f_k)\right\|_2 \le \|\mathbf{W}_x(f_k)\|_2\left\|\widehat{\mathbf{G}}_{s_0}(f_k)\right\|_2 \le \sqrt{N_r N_s}\|\mathbf{W}_x(f_k)\|_{\max}\left\|\widehat{\mathbf{G}}_{s_0}(f_k)\right\|_2. \tag{13}$$

So, Eqn. (11) can be relaxed as:

$$\sqrt{N_r N_s}\|\mathbf{W}_x(f_k)\|_{\max}\left\|\widehat{\mathbf{G}}_{s_0}(f_k)\right\|_2 \leq \min\{1-\epsilon_s, 1/B(f_k)\}. \tag{14}$$

If Eqn. (14) is satisfied, then Eqn. (11) will be satisfied because of the property shown in Eqn. (13). So the following constraint (Eqn. (15)), which can be formulated equivalently to a SOC, is able to replace Eqn. (1.d) and Eqn. (1.e):

$$\|\mathbf{W}_x(f_k)\|_{\max} \leq \frac{\min\{1-\epsilon_s, 1/B(f_k)\}}{\sqrt{N_r N_s}\left\|\widehat{\mathbf{G}}_{s_0}(f_k)\right\|_2}. \tag{15}$$

Alternatively, a relatively less conservative relaxation is to consider the Frobenius norm properties:

$$\left\|\mathbf{W}_x(f_k)\widehat{\mathbf{G}}_{s_0}(f_k)\right\|_2 \leq \left\|\mathbf{W}_x(f_k)\widehat{\mathbf{G}}_{s_0}(f_k)\right\|_F. \tag{16}$$

where

$$\left\|\mathbf{W}_x(f_k)\widehat{\mathbf{G}}_{s_0}(f_k)\right\|_F = \sqrt{\mathrm{tr}\left(\mathbf{W}_x(f_k)\widehat{\mathbf{G}}_{s_0}(f_k)\widehat{\mathbf{G}}_{s_0}(f_k)^{\mathrm{H}}\mathbf{W}_x(f_k)^{\mathrm{H}}\right)}. \tag{17}$$

Thus, the following constraint (Eqn. (18)), which can also be formulated equivalently to a SOC, is able to replace Eqn. (1.d) and Eqn. (1.e) as well:

$$\mathrm{tr}\left(\mathbf{W}_x(f_k)\widehat{\mathbf{G}}_{s_0}(f_k)\widehat{\mathbf{G}}_{s_0}(f_k)^{\mathrm{H}}\mathbf{W}_x(f_k)^{\mathrm{H}}\right) \leq \min\{(1-\epsilon_s)^2, 1/B(f_k)^2\}. \tag{18}$$

The ANC performance results using these two proposed relaxation methods, Eqn. (15) and Eqn. (18), will be compared in the Sec. 3.

3 Results

An ANC system installed on the wind channel of a central air handling system was used as the experimental setup. The experimental setup and its dimension are shown in Fig. 5 and Fig. 6. There were two speakers (served as secondary sources), four reference microphones and four error microphones in this system. The experimental setup is the same as in the referenced work[4]. The controller sampling rate is chosen to be 4 kHz. The filter length in each controller channel is 64. SDPT3[15] was used for testing the warmstarting performance because setting the initial point in SDPT3 is relatively easier compared with other software packages.

3.1 Comparison of Different Proposed Relaxation Methods

The noise control performance using different proposed relaxation methods were compared: (1) using the original PSD cones (Eqn. (1.d) and Eqn. (1.e)); (2) using Eqn. (15) which is referred to as method 1 in this section; and (3) using Eqn. (18) which is referred to as method 2 in this section. The noise control performance comparison is shown in Fig. 7, and the comparison of the value of $\max\left(\mathrm{Re}\left\{\lambda\left(-\mathbf{W}_x(f_k)\widehat{\mathbf{G}}_{s_0}(f_k)\right)\right\}\right)$ is shown in Fig. 8. ϵ_s is set to be 0.01, so the value of $\max\left(\mathrm{Re}\left\{\lambda\left(-\mathbf{W}_x(f_k)\widehat{\mathbf{G}}_{s_0}(f_k)\right)\right\}\right)$ should be less than 0.99 to be considered as stable. Parameter B is chosen to be 0.1 because the multiplicative plant uncertainty is less than 10%. The performance line (labelled "Original PSD") demonstrates the noise control performance when using the original PSD cones constraints solved by either the convex optimization method or traditional constrained optimization method. The main differences between using the convex optimization and the traditional constrained optimization are computational efficiency[4] and numerical stability[7] which can be referred to Zhuang and

Liu's previous work[4,7]. It can be observed from Fig. 7 that, compared with the proposed relaxation method 1, the proposed relaxation method 2 has a much better noise control performance especially from 1.2 kHz to 1.5 kHz. This result can be confirmed from Fig. 8. All three methods have stable filter design result because the $\max\left(\mathrm{Re}\left\{\lambda\left(-\mathbf{W}_x(f_k)\widehat{\mathbf{G}}_{s_0}(f_k)\right)\right\}\right)$ values of all three methods are less than 0.99. The method using original PSD cones has values very close to 0.99 from 1.2 kHz to 1.5 kHz, and the proposed relaxation method 2 has closer values to the original PSD cones case compared with the proposed relaxation method 1. This demonstrated that the proposed relaxation method 1 is a more conservative relaxation compared with method 2. Therefore, for the investigation of warmstarting method in the Subsec. 3.2, method 2 will be used for SOC only case.

3.2 Investigation of Warmstarting Method Performance

To investigate the warmstarting method performance, a series of perturbed problems were generated from the measured reference signal. Three cases of perturbation are considered: (a) perturbation of reference signal $\mathbf{S}_{xx}$; (b) perturbation of secondary path responses $\mathbf{G}_e$; and (c) perturbation of acoustical feedback path responses $\mathbf{G}_{s_0}$. The perturbed system responses for those three cases are generated using equations:

$$\mathbf{S}_{xx}^{\text{new}} = \mathbf{S}_{xx} \odot \left(\mathbf{E}_{N_r,N_r} + \frac{\alpha}{2}\left(\mathbf{P}_{N_r,N_r} + \mathbf{P}_{N_r,N_r}^{\mathrm{T}}\right)\right), \tag{19.a}$$

$$\mathbf{G}_e^{\text{new}} = \mathbf{G}_e \odot \left(\mathbf{E}_{N_e,N_s} + \alpha\, \mathbf{P}_{N_e,N_s}\right), \tag{19.b}$$

$$\mathbf{G}_{s_0}^{\text{new}} = \mathbf{G}_{s_0} \odot \left(\mathbf{E}_{N_r,N_s} + \alpha\, \mathbf{P}_{N_r,N_s}\right), \tag{19.c}$$

where $\mathbf{S}_{xx}^{\text{new}}$, $\mathbf{G}_e^{\text{new}}$, and $\mathbf{G}_{s_0}^{\text{new}}$ denote the cross spectral density matrix of the reference signal, secondary path response matrices, and acoustical feedback path response matrices in the perturbed problems for three different cases, respectively; $\mathbf{S}_{xx}$, $\mathbf{G}_e$, and $\mathbf{G}_{s_0}$ are measured from the experimental setup and used in the "original optimization problem" whose optimal solution will be noted as $\vec{\mathbf{x}}_p^*$, $\vec{\mathbf{s}}_d^*$, and $\vec{\mathbf{y}}_d^*$. $\odot$ denotes the Hadamard product (element-wise product). $\mathbf{E}_{m\times n}$ denotes an $m \times n$ matrix with all elements being 1. $\mathbf{P}_{m,n}$ is an $m \times n$ matrix with each element generated from a standard Gaussian process. α denotes the perturbation ratio as a measure of how much the problem is changed. It is noted that, the representation of perturbation in Eqn. (19.a) is different from that in Eqn. (19.b) and (19.c) because $\mathbf{S}_{xx}^{\text{new}}$ should always be positive semidefinite. Thus, the perturbation for $\mathbf{S}_{xx}^{\text{new}}$ should be symmetric. In this section, three different α values are used: 0.1%, 1%, and 5% to investigate the warmstarting performance under different perturbation level. Two different ANC formulations were investigated: (1) the original convex formulation Eqn. (1.a)-(1.e) (denoted as mixed SOC and PSD cones); and (2) the problem using proposed relaxation method 2, i.e., Eqn. (1.d) and Eqn. (1.e) are replaced by Eqn. (18) (denoted as SOC only). Seven different values of warm ratio g are used: 0.8, 0.9, 0.99, 0.999, 0.9999, 0.99999, and 0.999999. For each perturbation type, perturbation ratio, formulation, and warm ratio combination, 10 different perturbed problems are generated randomly, and the numbers of iterations needed to solve the filter design optimization problems are compared. It is noted that the number of iterations is used instead of the solving time because the computation time for each iteration in similar problems is usually the same[18] while the total solving time may be affected by the number of cores, or threads used in computers.

The warmstarting performance is compared in Fig. 9 to Fig. 14. Those figures show the mean and standard deviation of the iteration ratio (i.e., the ratio of the number of iterations using warmstarting method to the number of iterations using cold start method) for SOC only cases (proposed relaxation method 2) or mixed SOC and PSD cones cases (original formulation when proposed relaxation method is not used) when using different warm ratio g in Eqn. (10) and perturbation ratio α in Eqn. (19.a)-(19.c). From all six figures, when proposed SOC only relaxation method 2 was used, the warmstarting method can effectively reduce the required number of iterations using appropriate warm ratio (e.g., 0.999). However, if the proposed relaxation method is not applied to convert PSD cones into SOC (i.e., using the original formulation when proposed relaxation method is not used), the warmstarting method cannot have satisfactory result (the iterations ratios are around 1 or even larger than 1). This demonstrated that the proposed relaxation method 2 is essential to ensure the warmstarting method can work properly. It is shown as expected that the smaller the perturbation ratio is (i.e., the closer the new problem is to the original problem), the better the warmstarting method performs. When the perturbation ratio is about 0.1%, warmstarting ratio of 0.999 can achieve more than 60% of reduction in iterations for all SOC only cases, which significantly reduces the required computational effort of designing ANC filter. Even at relatively high perturbation ratio (5%), the warmstarting method can still reduce about 60% of the iterations for changing the secondary path $\mathbf{G}_e$ and the acoustic feedback path $\mathbf{G}_{s_0}$ cases and reduce about 20% of the iterations for changing the primary signal spectral cases. Fig. 9 to Fig. 14 also show that when warm ratio is too close to 1 (e.g., larger than 0.9999), the resulted initial points are too close to the boundaries and the required iterations are actually increasing with the increase of warm ratio g. The warm ratio higher than 0.999999 is not shown because it will then be highly likely outside the boundaries of constraint functions and cannot be used as initial point.

Another conclusion from Fig. 9 to Fig. 14 is that the standard deviation of iteration ratios is also small for most cases when an appropriate warm ratio is used such as 0.999. In some small perturbation cases (e.g., 0.1% or 1%), the reduction ratio is almost the same for randomly generated 10 cases, so the standard deviation is approximately 0 as shown in Fig. 11 – Fig. 14. This means that the warmstarting method is relatively reliable for different problems with similar environmental settings. This finding also confirms with the conclusions in previous literature that the required iteration is insensitive to the variation in data sets if they are from similar environmental settings[4,18]. This result further demonstrates the importance of the proposed warmstarting strategies because the reduction in iterations cannot achieved by simple methods such as data set tuning while the proposed warmstarting strategy can effectively and reliably achieve this reduction in iteration numbers. It is noted that the ANC performance will not be affected by using the warmstarting method compared with using cold start method because the ANC filter design formulation is convex. This is confirmed in Fig. 15 that the ANC performance is the same for using cold start and using warmstarting points of two different warm ratios.

4 Conclusions

In this article, the warmstarting strategies for constrained ANC optimal filter design problem is investigated. First, two relaxation methods are proposed to convert the original ANC design problem (i.e., mixed PSD and SOC problem) to a SOC-only problem. Results show that the relaxation method 2 (i.e., the relaxation of stability and robustness constraints using Frobenius norm properties) has better

noise control performance compared with the relaxation method 1 (i.e., the relaxation of stability and robustness constraints using max-norm properties).

Then, the warmstarting performance is compared between different problem types, warm ratios, and perturbation ratios. Several important conclusions can be drawn: a) the proposed relaxation method 2 is essential to ensure the warmstarting method can work properly; b) one appropriate chosen warm ratio (i.e., 0.999 in the setup in this article), can achieve more than 60% reduction on most of the cases with different types or levels of perturbation to the original problem which means the method is effective and robust in various different environmental setup and there is no need for mass tuning efforts; c) as long as the proposed relaxation method 2 is applied, the warmstarting method can achieve better efficiency compared with using the cold start point for a wide range of warm ratios (0.8 – 0.9999). These results demonstrated that the used warmstarting method combined with the proposed constraint relaxation can be used effectively and reliably in ANC applications. Practically, this is helpful for commercial product development that involves designing ANC filter in similar but different environmental setups.

5 ACKNOWLEDGMENTS

The authors thank Beijing Ancsonic Technology Co. Ltd for providing financial support and help on the experimental system setup and data collection related to the presented work.

6 REFERENCES

1. Elliott SJ. *Signal Processing for Active Control*. Academic Press; 2001. http://www.sciencedirect.com/science/article/pii/B9780122370854500089

2. Shi D, Gan WS, Lam B, Wen S, Shen X. Optimal output-constrained active noise control based on inverse adaptive modeling leak factor estimate. *IEEEACM Trans Audio Speech Lang Process*. 2021;29:1256-1269.

3. Shi D, Gan WS, Lam B, Shen X. Comb-partitioned frequency-domain constraint adaptive algorithm for active noise control. *Signal Process*. 2021;188:108222.

4. Zhuang Y, Liu Y. Constrained optimal filter design for multi-channel active noise control via convex optimization. *J Acoust Soc Am*. 2021;150(4):2888-2899.

5. Zhuang Y, Liu Y. Study on the Cone Programming Reformulation of Active Noise Control Filter Design in the Frequency Domain. In: *INTER-NOISE and NOISE-CON Congress and Conference Proceedings*. Vol 260. Institute of Noise Control Engineering; 2019:126-136.

6. Zhuang Y, Liu Y. Development and Application of Dual Form Conic Formulation of Multichannel Active Noise Control Filter Design Problem in Frequency Domain. In: *INTER-NOISE and NOISE-CON Congress and Conference Proceedings*. Vol 261. Institute of Noise Control Engineering; 2020:676-687.

7. Zhuang Y, Liu Y. A numerically stable constrained optimal filter design method for multichannel active noise control using dual conic formulation. *J Acoust Soc Am*. 2022;152(4):2169-2182.

8. Sturm JF. Implementation of interior point methods for mixed semidefinite and second order cone optimization problems. *Optim Methods Softw*. 2002;17(6):1105-1154.

9. Tütüncü RH, Toh KC, Todd MJ. SDPT3—a Matlab software package for semidefinite-quadratic-linear programming, version 3.0. Published online August 21, 2001. https://www.math.cmu.edu/~reha/Pss/guide3.0.pdf

10. Xia Y. *An Algorithm for Perturbed Second-Order Cone Programs*. Advanced Optimization Laboratory, McMaster University; 2004.

11. Gondzio J, Grothey A. A new unblocking technique to warmstart interior point methods based on sensitivity analysis. *SIAM J Optim*. 2008;19(3):1184-1210. doi:10.1137/060678129

12. Skajaa A. *The Homogeneous Interior-Point Algorithm: Nonsymmetric Cones, Warmstarting, and Applications*. Technical University of Denmark; 2013.

13. Skajaa A, Andersen ED, Ye Y. Warmstarting the homogeneous and self-dual interior point method for linear and conic quadratic problems. *Math Program Comput*. 2013;5(1):1-25.

14. Zhuang Y, Mo Z, Liu Y. Warmstarting the constrained optimal filter design problem for active noise control systems in conic formulation. In: *INTER-NOISE and NOISE-CON Congress and Conference Proceedings*. ; 2022:259-269. doi:https://doi.org/10.3397/NC-2022-727

15. Toh KC, Todd MJ, Tütüncü RH. On the implementation and usage of SDPT3--a Matlab software package for semidefinite-quadratic-linear programming, version 4.0. In: *Handbook on Semidefinite, Conic and Polynomial Optimization*. Springer; 2012:715-754.

16. Cheer J, Elliott SJ. Multichannel control systems for the attenuation of interior road noise in vehicles. *Mech Syst Signal Process*. 2015;60:753-769.

17. Rafaely B, Elliott SJ. ${H}_2$ / ${H}_{\infty}$ active control of sound in a headrest: design and implementation. *IEEE Trans Control Syst Technol*. 1999;7(1):79-84.

18. Boyd S, Vandenberghe L. *Convex Optimization*. Cambridge university press; 2004.

Table 1—A list of used variables

Variables	Definition
N_r	The number of reference sensors (i.e., the ANC controller input channels)
N_s	The number of secondary actuators (i.e., the ANC controller output channels)
N_e	The number of error sensors
$\vec{\mathbf{x}}$	The primary noise signals measured at reference sensor locations
$\vec{\mathbf{r}}$	The total measured signals at reference sensor locations
$\vec{\mathbf{y}}$	The outputs of the ANC controller
$\vec{\mathbf{d}}_e$	The disturbance signals
$\vec{\mathbf{e}}$	The error signals whose power is to be minimized
$\mathbf{G}_{s_0}$	The acoustic feedback path matrix from secondary speakers to reference sensors
$\mathbf{G}_e$	The acoustical response matrix from secondary speakers to error sensors
$\mathbf{W}_x$	The frequency response matrix of the multi-channel ANC FIR filters
$\mathbf{w}_F$	The multi-channel ANC FIR filter time-domain coefficients
$\vec{\mathbf{w}}$	A vector containing all filter coefficients in $\mathbf{w}_F$ and is defined in Eqn. (2)
f_k	The k-th frequency point
$i,\ j$	The controller output channel index i and input channel index j
$\mathbf{S}_{xx}, \mathbf{S}_{d_e d_e}$	The cross-spectral density matrix of $\vec{\mathbf{x}}$ and $\vec{\mathbf{d}}_e$ respectively
$\mathbf{S}_{xd_e}$	The cross-spectral density matrix of $\vec{\mathbf{x}}$ and $\vec{\mathbf{d}}_e$
$\vec{\mathbf{F}}_z$	The Fourier transform vector
$\mathbf{A}_J, \vec{\mathbf{b}}_J, \tilde{c}_J$	Defined using Eqn. (3.a), (3.b), and (4) respectively
A_e	The upper bound of disturbance enhancement (noise amplification) ratio of error signal
$C_{i,j}$	The upper bound of frequency response magnitude of designed control filter
$\mathbf{A}_s$	Defined using Eqn. (5)
ϵ_s	A small positive number to ensure strict inequality constraints
B	The upper bound of the output multiplicative plant uncertainty
$\vec{\mathbf{x}}_p$	Primal variables in conic ANC formulation
$\vec{\mathbf{y}}_d$	Dual variable associated with equality constraints in conic ANC formulation
$\vec{\mathbf{s}}_d$	Dual variable associated with inequality (conic) constraints in conic ANC formulation
$\mathbf{A}, \vec{\mathbf{b}}, \vec{\mathbf{c}}$	Denotes the matrix and vectors in ANC formulation for simplicity
g	Warm ratio
$\tau,\ \kappa,\ \theta$	Introduced variables when using the homogeneous and self-dual model
α	Perturbation ratio for simulating a perturbed problem
$\mathbf{E}_{m\times n}$	An $m \times n$ matrix with all elements being 1
$\mathbf{P}_{m,n}$	An $m \times n$ matrix with each element generated from a standard Gaussian process

List of Figure Captions

Fig. 1—An illustration of the difficulties of applying warmstarting strategies to primal-dual interior-point method.

Fig. 2—Block diagram of the MIMO feedforward controllers with the acoustic feedback path and internal model control structure4.

Fig. 3—Block diagram of the MIMO feedforward controllers in a standard feedforward form when assuming internal model control structure perfectly cancels the acoustic feedback path effect4.

Fig. 4—An illustration of the warmstarting strategies.

Fig. 5—The experimental setup[4]. The red arrows demonstrate the air flow direction.

Fig. 6—Dimension of the experimental setup (unit: mm)[4]. The red arrows demonstrate the air flow direction.

Fig. 7—The comparison of noise control performance between the originally used PSD cones robust stability constraints, relaxed SOC robust stability constraints using method 1, and relaxed SOC robust stability constraints using method 2.

Fig. 8—The comparison of the value of $\max\left(Re\left\{\lambda\left(-W_x(f_k)\hat{G}_{s_0}(f_k)\right)\right\}\right)$ *when using the originally used PSD cones robust stability constraints, relaxed SOC robust stability constraints using method 1, and relaxed SOC robust stability constraints using method 2.* ϵ_s *is set to be 0.01 and thus, the value should be less than 0.99 to be considered as stable.*

Fig. 9—The mean and standard deviation of iteration ratio (i.e., iterations using warmstarting method / iterations using cold start method) when using different warm ratio g *and perturbation ratio* α *on* S_{xx}*. Ten cases with SOC only (using proposed relaxation method 2) are randomly generated and tested for each combination of warm ratio and perturbation ratio.*

Fig. 10—The mean and standard deviation of iteration ratio (i.e., iterations using warmstarting method / iterations using cold start method) when using different warm ratio g *and perturbation ratio* α *on* S_{xx}*. Ten cases with mixed SOC and PSD cones (using original convex formulation) are randomly generated and tested for each combination of warm ratio and perturbation ratio.*

Fig. 11—The mean and standard deviation of iteration ratio (i.e., iterations using warmstarting method / iterations using cold start method) when using different warm ratio g *and perturbation ratio* α *on* G_e*. Ten cases with SOC only (using proposed relaxation method 2) are randomly generated and tested for each combination of warm ratio and perturbation ratio.*

Fig. 12—The mean and standard deviation of iteration ratio (i.e., iterations using warmstarting method / iterations using cold start method) when using different warm ratio g *and perturbation ratio*

α on G_e. Ten cases with mixed SOC and PSD cones (using original convex formulation) are randomly generated and tested for each combination of warm ratio and perturbation ratio.

Fig. 13—The mean and standard deviation of iteration ratio (i.e., iterations using warmstarting method / iterations using cold start method) when using different warm ratio g and perturbation ratio α on G_s. Ten cases with SOC only (using proposed relaxation method 2) are randomly generated and tested for each combination of warm ratio and perturbation ratio.

Fig. 14—The mean and standard deviation of iteration ratio (i.e., iterations using warmstarting method / iterations using cold start method) when using different warm ratio g and perturbation ratio α on G_s. Ten cases with mixed SOC and PSD cones (using original convex formulation) are randomly generated and tested for each combination of warm ratio and perturbation ratio.

Fig. 15—The comparison of noise control performance between using cold start initial point and warmstarting points using different warm ratio g.

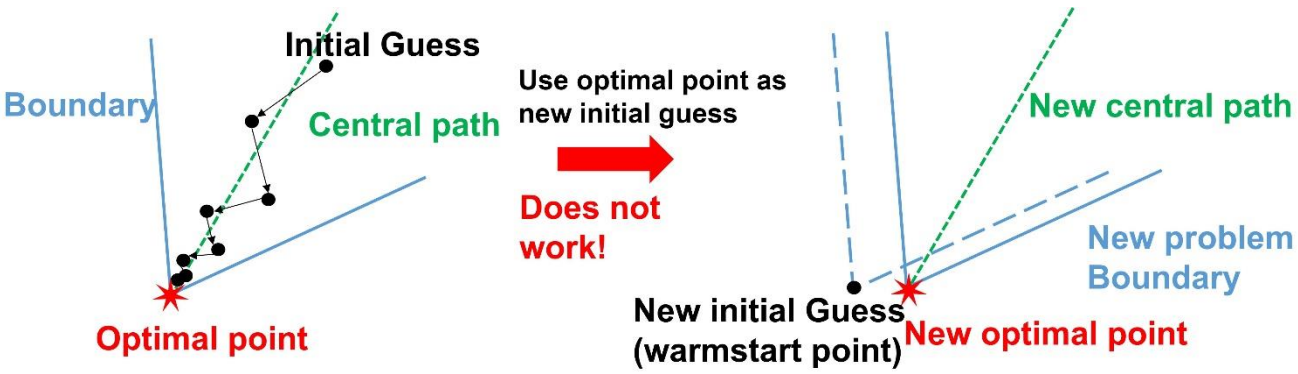

Fig. 1—An illustration of the difficulties of applying warmstarting strategies to primal-dual interior-point method.

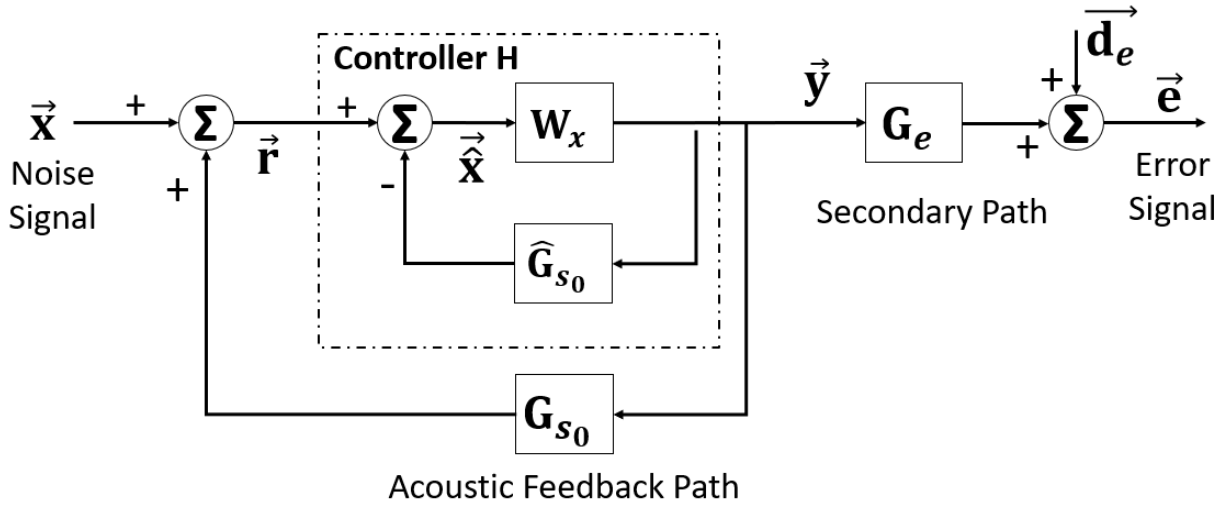

Fig. 2—Block diagram of the MIMO feedforward controllers with the acoustic feedback path and internal model control structure[4].

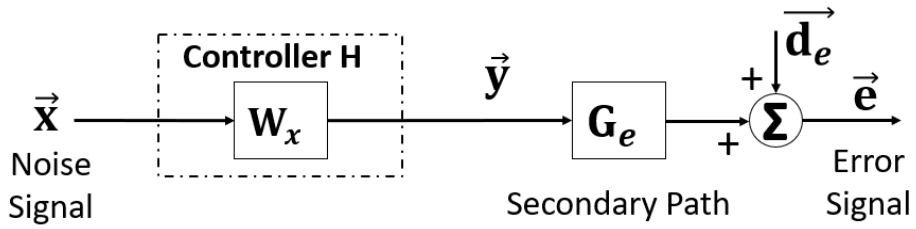

Fig. 3—Block diagram of the MIMO feedforward controllers in a standard feedforward form when assuming internal model control structure perfectly cancels the acoustic feedback path effect[4].

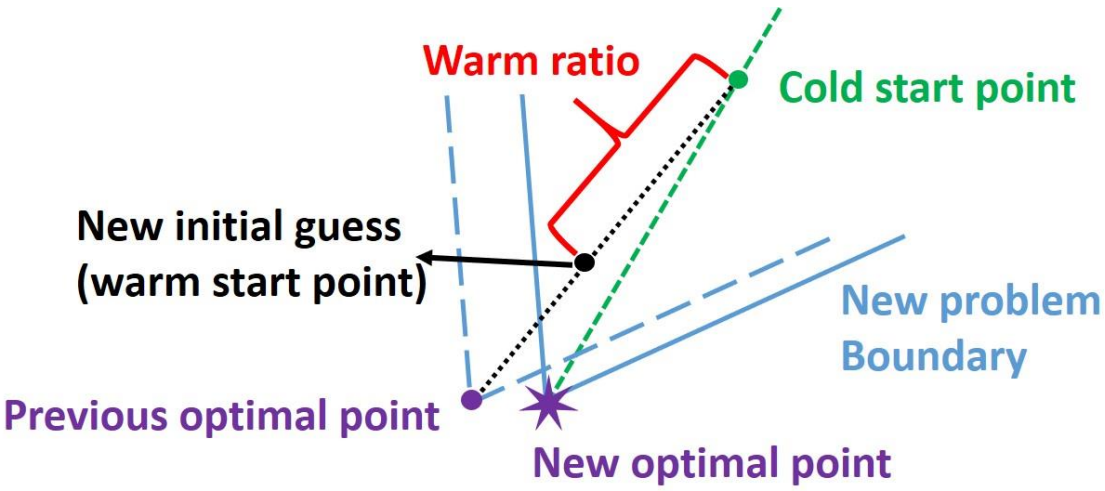

Fig. 4—An illustration of the warmstarting strategies.

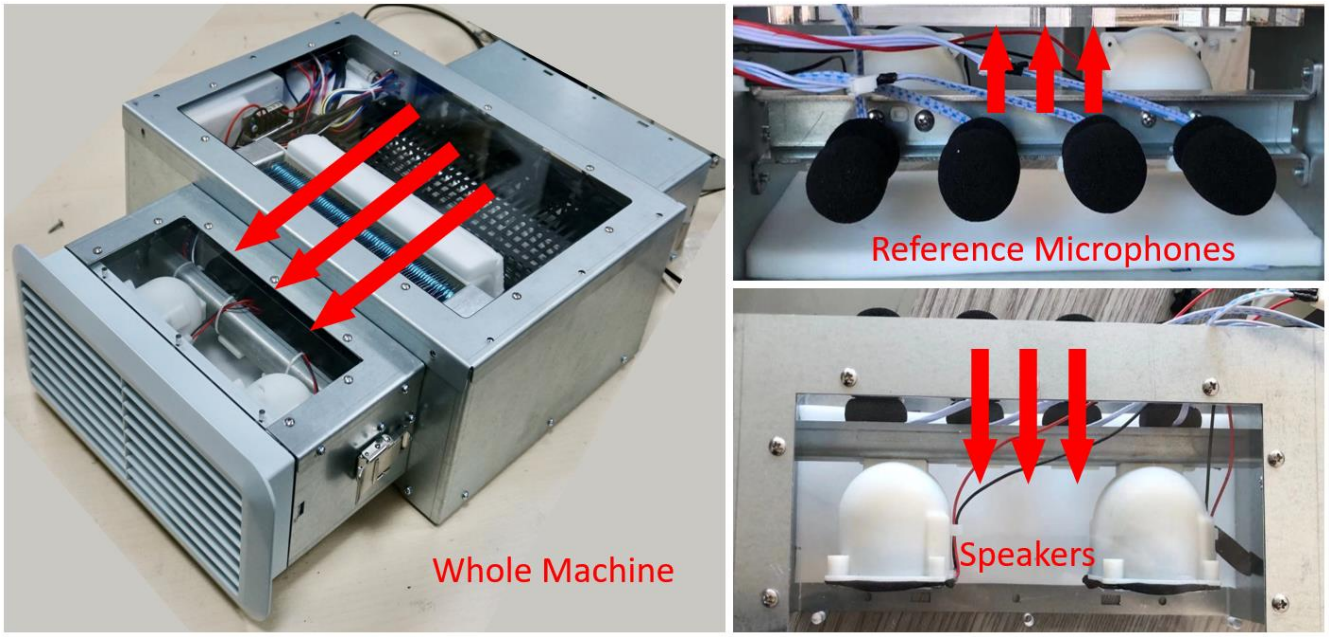

Fig. 5—The experimental setup[4]. The red arrows demonstrate the air flow direction.

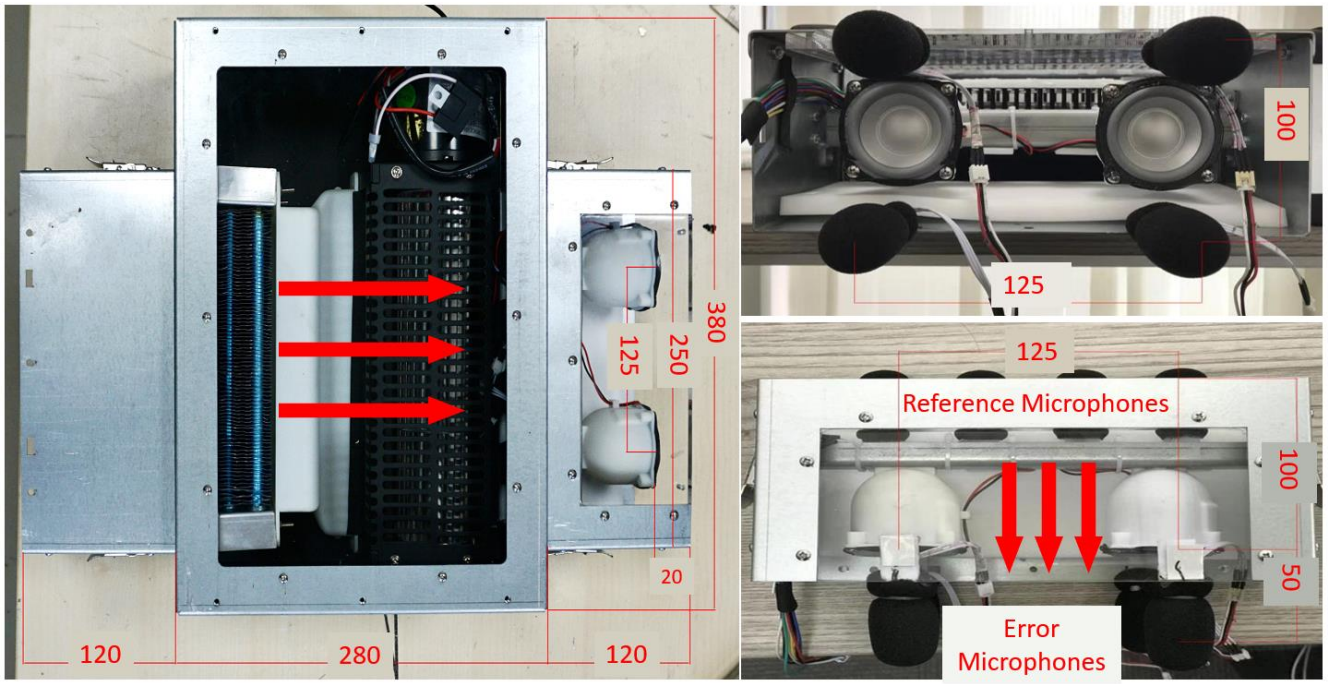

Fig. 6—Dimension of the experimental setup (unit: mm)[4]. The red arrows demonstrate the air flow direction.

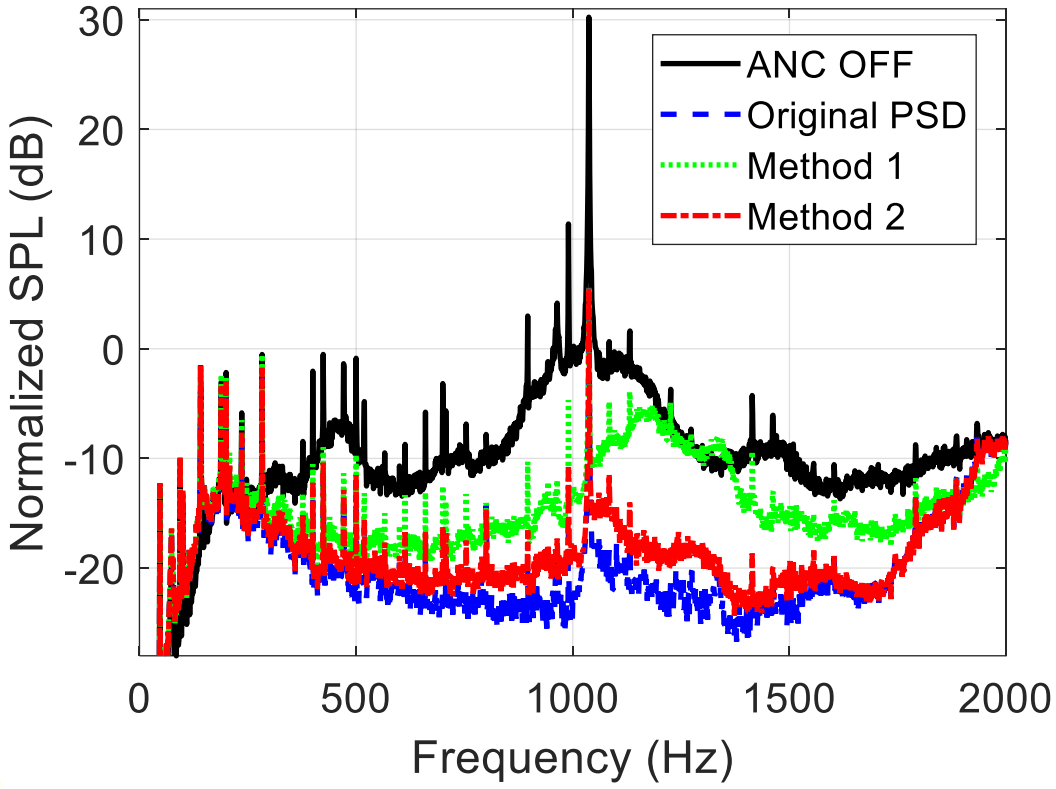

Fig. 7—The comparison of noise control performance between the originally used PSD cones robust stability constraints, relaxed SOC robust stability constraints using method 1, and relaxed SOC robust stability constraints using method 2.

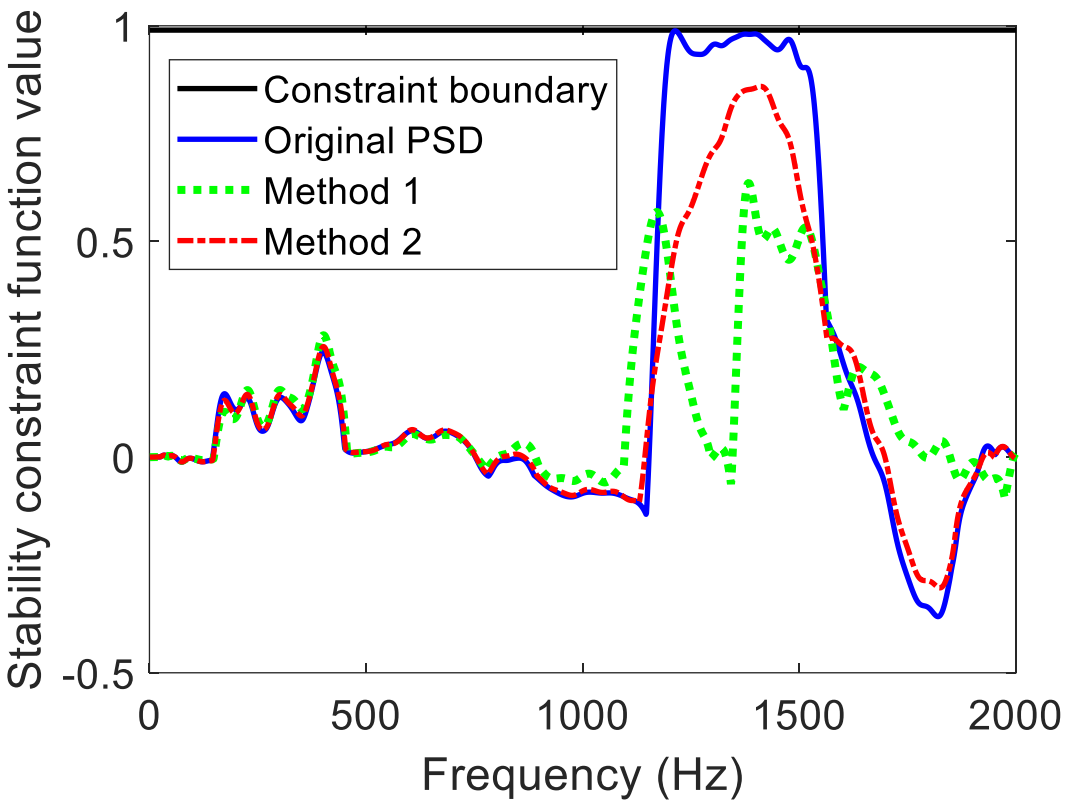

Fig. 8—The comparison of the value of $max\left(Re\left\{\lambda\left(-\boldsymbol{W}_x(f_k)\widehat{\boldsymbol{G}}_{s_0}(f_k)\right)\right\}\right)$ *when using the originally used PSD cones robust stability constraints, relaxed SOC robust stability constraints using method 1, and relaxed SOC robust stability constraints using method 2.* ϵ_s *is set to be 0.01 and thus, the value should be less than 0.99 to be considered as stable.*

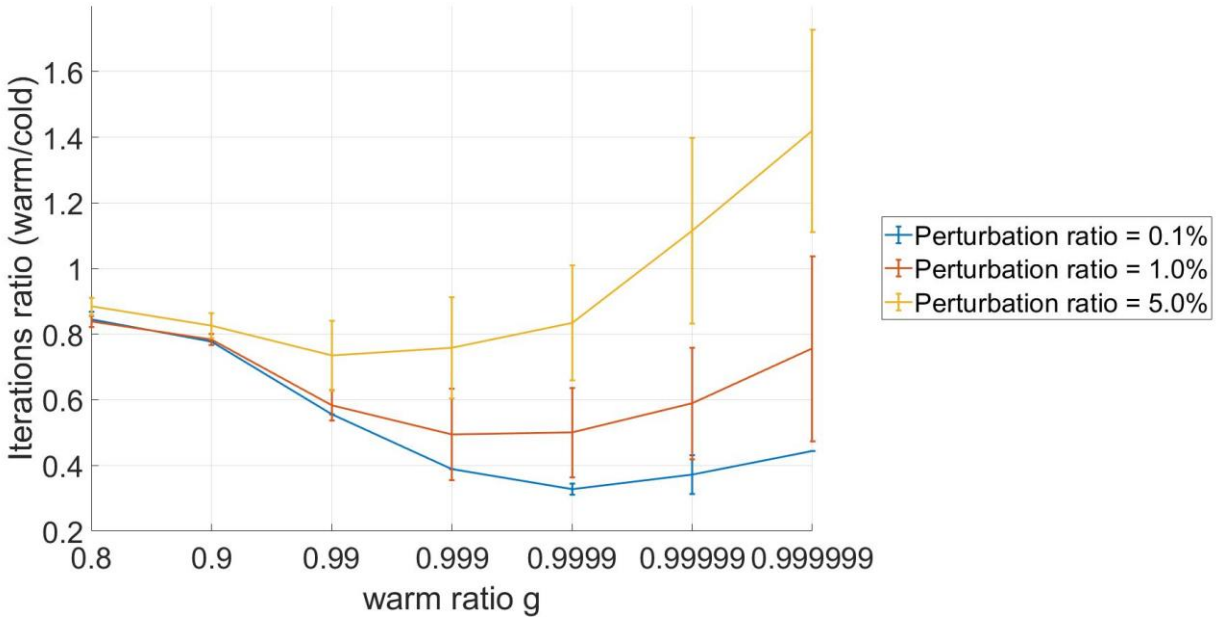

Fig. 9—The mean and standard deviation of iteration ratio (i.e., iterations using warmstarting method / iterations using cold start method) when using different warm ratio g and perturbation ratio α on $\boldsymbol{S}_{xx}$. Ten cases with SOC only (using proposed relaxation method 2) are randomly generated and tested for each combination of warm ratio and perturbation ratio.

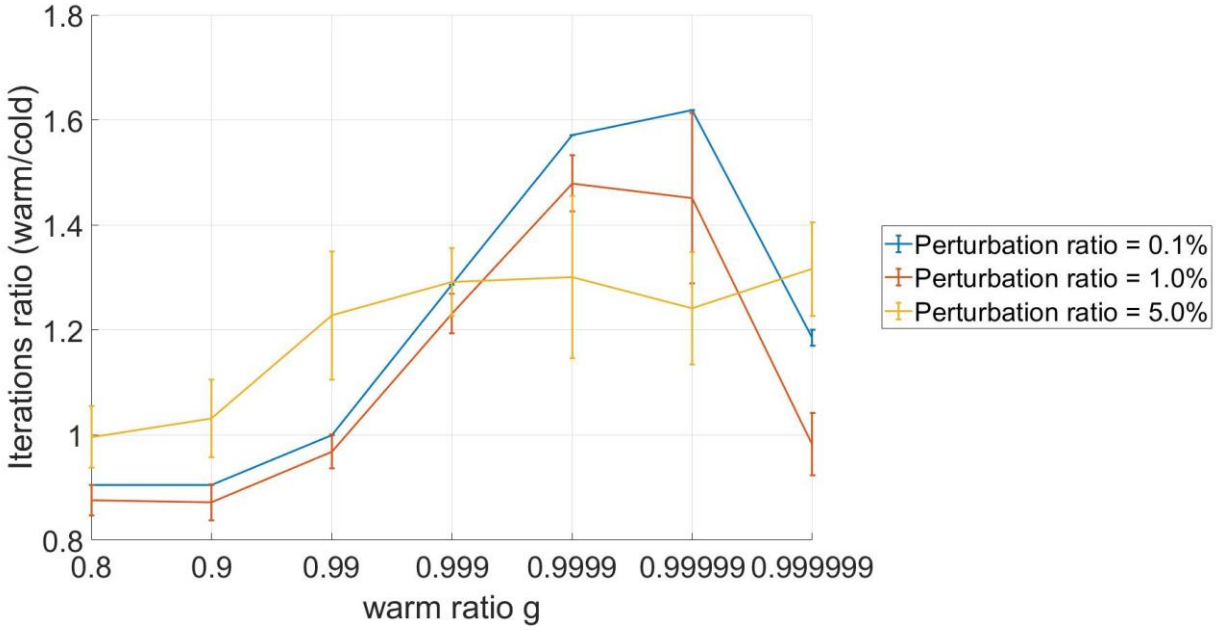

Fig. 10—The mean and standard deviation of iteration ratio (i.e., iterations using warmstarting method / iterations using cold start method) when using different warm ratio g and perturbation ratio α on $\boldsymbol{S}_{xx}$. Ten cases with mixed SOC and PSD cones (using original convex formulation) are randomly generated and tested for each combination of warm ratio and perturbation ratio.

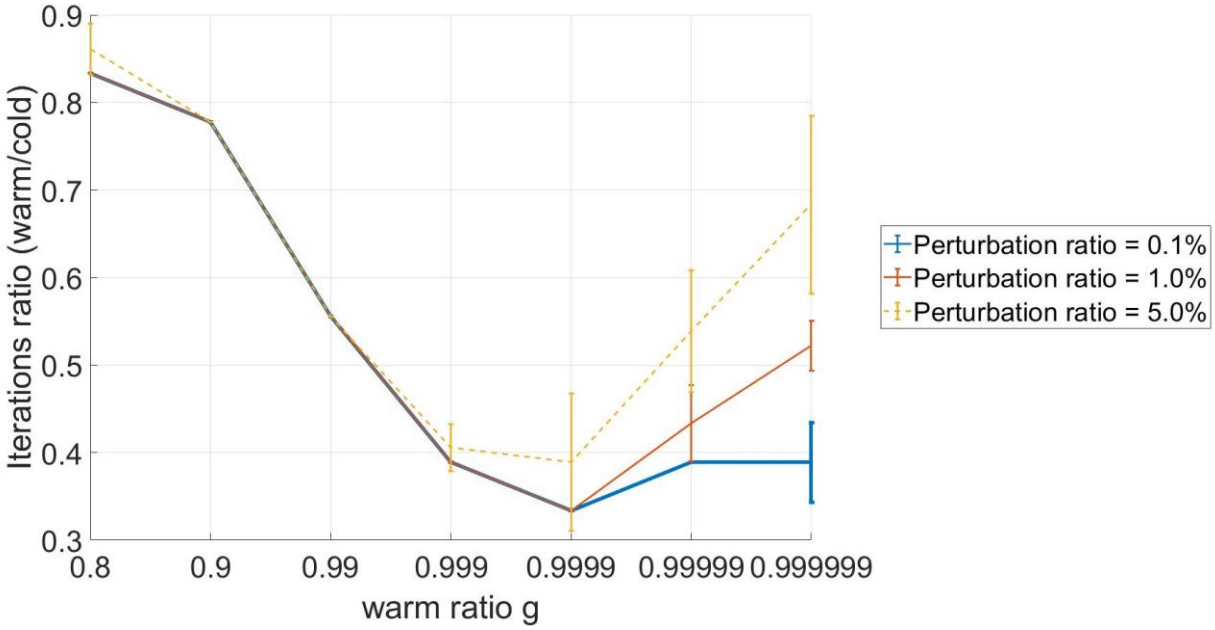

Fig. 11—The mean and standard deviation of iteration ratio (i.e., iterations using warmstarting method / iterations using cold start method) when using different warm ratio g and perturbation ratio α on $\boldsymbol{G}_e$. Ten cases with SOC only (using proposed relaxation method 2) are randomly generated and tested for each combination of warm ratio and perturbation ratio.

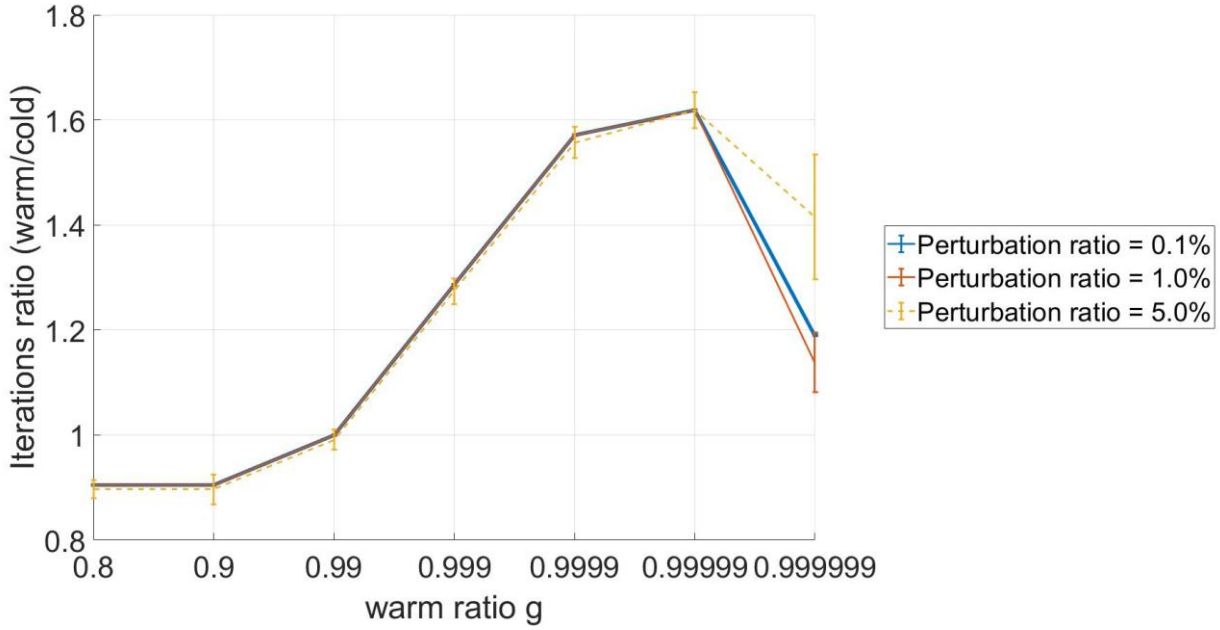

Fig. 12—The mean and standard deviation of iteration ratio (i.e., iterations using warmstarting method / iterations using cold start method) when using different warm ratio g and perturbation ratio α on $\boldsymbol{G}_e$. Ten cases with mixed SOC and PSD cones (using original convex formulation) are randomly generated and tested for each combination of warm ratio and perturbation ratio.

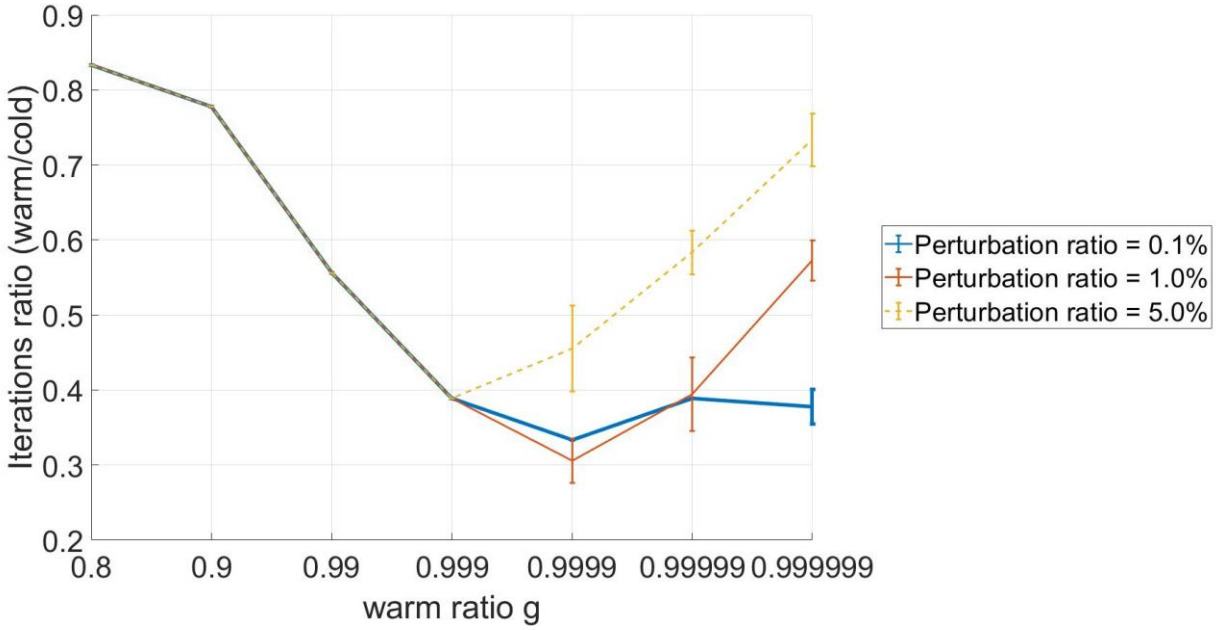

Fig. 13—The mean and standard deviation of iteration ratio (i.e., iterations using warmstarting method / iterations using cold start method) when using different warm ratio g and perturbation ratio α on $\boldsymbol{G}_s$. Ten cases with SOC only (using proposed relaxation method 2) are randomly generated and tested for each combination of warm ratio and perturbation ratio.

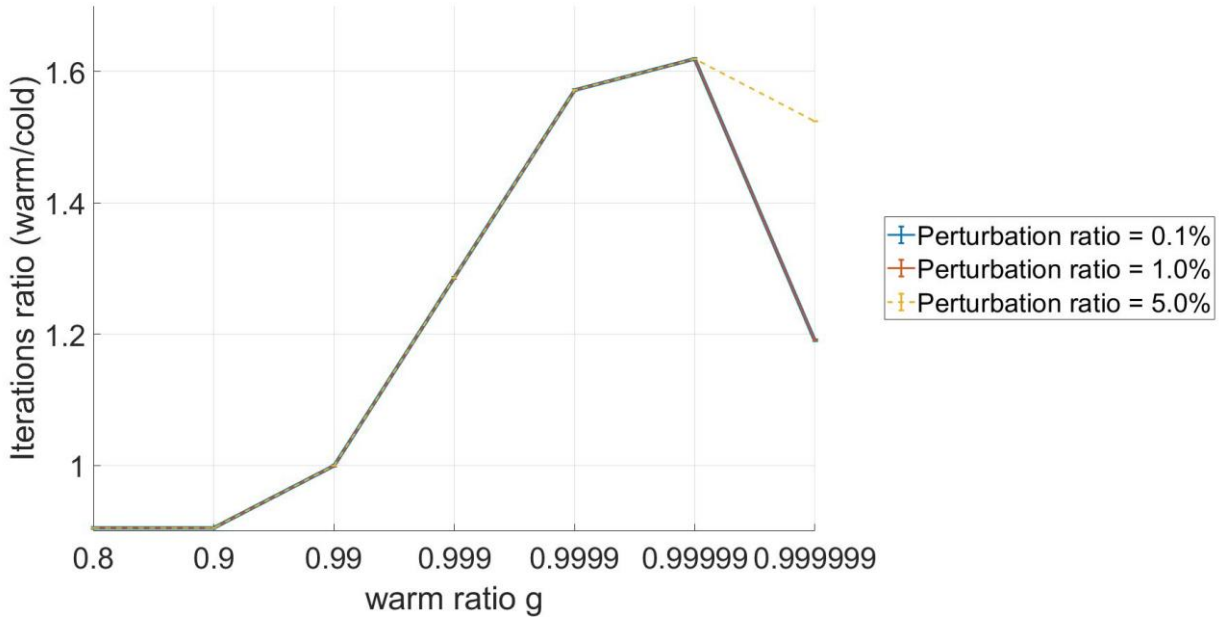

Fig. 14—The mean and standard deviation of iteration ratio (i.e., iterations using warmstarting method / iterations using cold start method) when using different warm ratio g and perturbation ratio α on $\boldsymbol{G}_s$. Ten cases with mixed SOC and PSD cones (using original convex formulation) are randomly generated and tested for each combination of warm ratio and perturbation ratio.

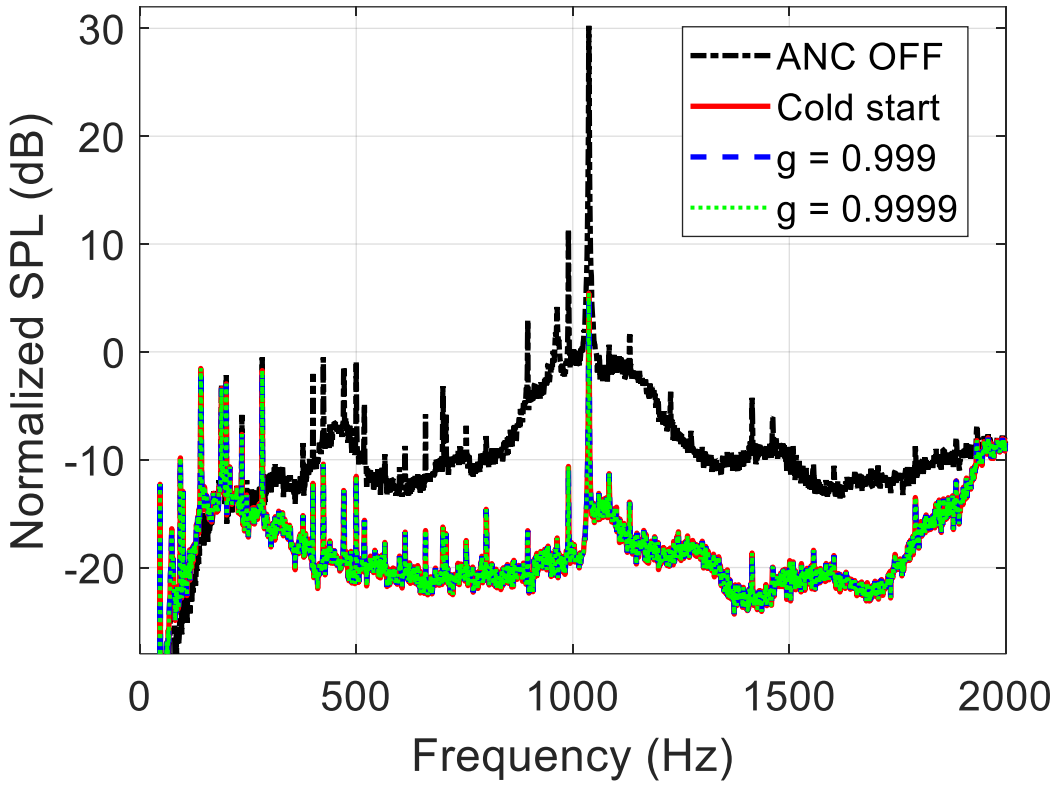

Fig. 15—The comparison of noise control performance between using cold start initial point and warmstarting points using different warm ratio g.